Diamond and β-SiC heteroepitaxial interfaces: A theoretical and experimental study

W. Zhu, X. H. Wang, B. R. Stoner, G. H. M. Ma,* H. S. Kong,† M. W. H. Braun,‡ and J. T. Glass

Department of Materials Science and Engineering, North Carolina State University, Raleigh, North Carolina 27695-7919

(Received 10 July 1992)

A comparative study of both theoretical and experimental aspects of the diamond/β-SiC heteroepitaxial interface was performed. The theoretical modeling was conducted to examine the various combinations of like and unlike interfacial planes between diamond and β-SiC based on a geometric criterion formulated in reciprocal space for minimization of interfacial misfit and strain energies. The modeling results indicated that the low-index unlike pair between diamond {114} and β-SiC {221} has the greatest potential for minimizing the interfacial energy and is, therefore, strongly recommended for experimental investigations. The low-index-like pairs between diamond and β-SiC are next in potential, and diamond (001)/β-SiC(001) heteroepitaxy has been confirmed via experimental observations. Other configurations yield high interfacial energies and are unlikely to occur. The relatively high strain energy associated with the like-pair heteroepitaxy can be relieved by the introduction of misfit dislocations at the interface. These misfit dislocations have also been experimentally observed by cross-sectional transmission electron microscopy. The calculated misfit dislocation densities correlate well with the experimental measurements. The misfit dislocations observed in diamond not only accommodate the misfit strain but also cause both interfacial tilting and azimuthal rotational misorientations.

I. INTRODUCTION

The heteroepitaxy of diamond via chemical-vapor deposition (CVD) is a process of considerable scientific and technological importance. Many applications of diamond, especially in the area of microelectronics, await the growth of single-crystal diamond on economically viable substrates. However, unlike the preparations of silicon, germanium and III-V semiconductor elements and compounds in which heteroepitaxial growth is a rather common practice, the successful two-dimensional heteroepitaxial growth of diamond films has not been documented despite several years of research using a wide variety of substrates. There is a general lack of scientific understanding of the nucleation mechanisms of diamond under CVD conditions. This, in turn, hinders the development of pertinent techniques in areas such as substrate surface preparation and interface engineering. Single-crystal diamond films necessary for electronic device applications have only been grown homoepitaxially on diamond substrates.

There is some evidence, however, that diamond can be grown epitaxially on micrometer-sized cubic boron nitride (cBN) crystals.[1-3] Cubic boron nitride has been considered an ideal substrate for diamond heteroepitaxy because of its close lattice-parameter match with diamond [1.3% as defined by $(a_s - a_0)/a_s$, where a_s and a_0 are lattice constants of the substrate and overgrowth, respectively] and its high surface energy (~ 4.8 J/m^2 for the {111} planes).[4] Unfortunately, cBN substrates of sufficient size to make the diamond growth process practical are unavailable at the present time. Therefore, substrate candidates other than cBN must be considered. Some additional experiments included the use of Si, Ni, Cu, and a few refractory metals such as W, Mo, and Ta.[5-11] Although there was limited evidence of local epitaxy of diamond on some of these materials, such as Si and Ni,[5-8] most of the experiments yielded randomly oriented, island growth of diamond.

The reason for the difficulty in achieving diamond heteroepitaxy is believed to be largely due to its high surface energy[12] (in the range of 5.3–9.2 J/m^2 for the principal low-index planes) and small interatomic spacing, which prevents diamond from forming oriented, two-dimensional nuclei on a foreign substrate surface. Random nucleation of diamond starts at numerous sites on the substrate, which subsequently leads to three-dimensional island growth and forms a polycrystalline film. In addition, both misfit and strain energies at the interface enhance the tendency toward three-dimensional growth when the lattice mismatch between diamond and the substrate is significant. Careful and correct selection of the substrate, its surface preparation and *in situ* interface engineering are, therefore, critical in overcoming these energy barriers and achieving diamond heteroepitaxy.

The use of cubic silicon carbide (β-SiC) as a substrate for diamond heteroepitaxial growth has long been of interest. The idea originated from the observations that a silicon carbide interfacial layer exists between the diamond film and silicon substrate, and any observed local epitaxy of diamond on a Si substrate (34% lattice-parameter mismatch between diamond and Si) is most likely a result of limited diamond epitaxial growth on the interfacial silicon carbide layer.[5-7] Although the 18% lattice-parameter mismatch between diamond ($a = 3.57$ Å) and β-SiC ($a = 4.36$ Å) may cause problems in the control of growth orientations and defect genera-

tion in the diamond, there are numerous examples in preparations of other semiconductor materials as well as metal-semiconductor structures such as CdTe/GaAs,[13] β-SiC/Si,[14] Al/Si,[15] and Ag/Si,[16] where proper growth techniques were developed to accommodate significant lattice-parameter mismatches (ranging from 14.6% for CdTe/GaAs to 25% for Ag/Si) between the overgrowths and substrates while still maintaining the epitaxial relationship. The most notable and relevant case is the heteroepitaxial growth of β-SiC on Si substrates (a mismatch in lattice parameters of 20% between β-SiC and Si). Methods were developed for the reduction of mismatch via the initial reaction of the Si surface with a carbon-containing gas which produced a converted layer upon which SiC films could be epitaxially grown.[17,18] Further development of the growth techniques has dramatically lowered the defect density via growth on off-axis Si surfaces or hexagonal SiC (α-SiC) {0001} surfaces and resulted in the successful fabrication of commercially viable electronic devices.[14,19,20]

These documented experiments of β-SiC deposition on Si clearly indicate that the lattice-parameter mismatch between diamond and β-SiC is not a prohibiting factor for heteroepitaxy. However, earlier reports on the growth of diamond on bulk β-SiC single crystals have not been encouraging.[21,22] It was found that the initial nucleation of diamond on a clean, undamaged β-SiC surface was not possible. This problem was recently alleviated by Stoner and Glass[23] utilizing an *in situ* dc biasing technique to enhance the nucleation density of diamond on the β-SiC substrate in a microwave plasma CVD system. They found that over fifty percent of the diamond nuclei showed epitaxial orientation with the (001)-oriented β-SiC substrate. This is a rather encouraging development in the diamond/β-SiC heteroepitaxial system and deserves careful theoretical and experimental attention.

The purpose of this paper is to perform a comparative study of both theoretical and experimental aspects of the diamond/β-SiC heteroepitaxial interface to gain a better understanding of this system and thus enable further progress in diamond heteroepitaxy. Detailed studies of the misfit and strain energies, atomic structures, defects, and orientational relationships at the heteroepitaxial interface were conducted. Specifically, the various combination of low-index, like and unlike, interfacial planes between diamond and β-SiC were examined based on a geometric criterion formulated in reciprocal space for minimization of interfacial energy when crystals grow together on a planar epitaxial interface. The energies involved in the many possible interfacial configurations between diamond and β-SiC were evaluated. Conditions were formulated under which the tendency for a system to promote epitaxial growth can be ranked, and the most energetically favorable epitaxial configuration was predicted. A detailed experimental characterization of a (001) diamond/β-SiC interfacial registry, defects, and orientational relationship by high-resolution electron microscopy and electron diffraction was also performed. These experimental observations of the heteroepitaxial interface are correlated with the theoretical results in order to assess the usefulness of the theory. In addition, the generation of misfit dislocations at the interface is discussed in an effort to understand the roles of dislocations in the reduction of interfacial strain energy and in the development of epitaxial orientations. Future research directions leading to improved two-dimensional heteroepitaxy of diamond on β-SiC are also discussed. It is believed that the results obtained from this theoretical and experimental investigation will allow us to better understand the atomic structures of the diamond/β-SiC heteroepitaxial interface, the associated interfacial energies, and the nucleation mechanisms leading to the epitaxial orientations. The acquired knowledge will also provide useful guidelines for further development of the relevant growth techniques.

The paper will first provide a brief review of the theory of heteroepitaxial interfaces which is employed here for the examination of the diamond/β-SiC heteroepitaxial system. It will then present the calculated results of the interfacial strain energy and the corresponding misfit configurations between diamond and β-SiC and make useful predictions of the favorable interfacial planes for epitaxy based on the theoretical considerations. Next, high-resolution electron micrographs of the diamond/β-SiC interface and the corresponding electron-diffraction pattern will be presented. The experimental observations such as misfit dislocations and interfacial tilt will be correlated with the modeling results. It will be seen that the correlations between the interface theory and experimental observations are very encouraging, and the theoretical model is a useful tool for evaluating and selecting candidate systems for heteroepitaxial growth.

II. THEORY OF HETEROEPITAXIAL INTERFACES

A heteroepitaxial system consists of a single-crystal substrate bonded to a single-crystal overgrowth of a different chemical composition at a common interface, the crystal lattice of the overgrowth having a definite orientation with respect to the lattice of the substrate. Due to the lattice mismatch between the two crystals involved, there is an excess interfacial energy associated with the creation of the heteroepitaxial interface. Assuming that the substrate is thick and rigid, and the overgrowth is thin and deformable, this interfacial energy normally contains the competing elastic strain energy in the overgrowth and the misfit energy resulting from the interfacial disregistry between the two lattices. Theories of such heteroepitaxial interfaces have been advanced to find the criteria for ideal epitaxial configurations and to estimate the tendency to epitaxy for various systems.[24–29] The overwhelming task of these theoretical treatments is to accurately calculate the interfacial energy and its dependence on the fit of the two atomic planes at the interface. Although it has not, in general, been possible to make quantitative predictions by these theoretical models, qualitative predictions on epitaxial orientations and/or interfacial structures have correlated satisfactorily with experimental results.

The present research will utilize an epitaxial criterion formulated in reciprocal space first developed by Fletch-

er[25,26] and later extended and generalized by Braun[30,31] to analyze the diamond/β-SiC heteroepitaxial system. The principles of the interfacial energy considerations are based on the rigid models proposed by Reiss[27] and Van der Merwe.[28] In their models, it is assumed that both the overgrowth and substrate are rigid, retain their bulk lattice structures and parameters and elastic properties, and are in contact at a chemically abrupt and atomically smooth interfacial plane. Thus, the crystal on either side of the interface presents a plane with unique translational and rotational symmetries and can be described by infinite sets of wave vectors which form the surface reciprocal lattices of each crystallographic plane. A geometric epitaxial criterion related to the matching of rows of atoms on either side of the interface by minimizing the interfacial energy is subsequently developed based on the reciprocal sets of vectors.

The main assumption in this theoretical analysis is that epitaxial orientations minimize the interfacial energy. To calculate the energy of an interface between two crystals, it is important to know the interaction potential between the substrate and overgrowth atoms and the elastic moduli of the two crystals. Several models are available to carry out this calculation subject to various approximations. For example, Fletcher[25] and Fletcher and Lodge[26] calculated the interaction potential (or interaction energy) by summing over all the interatomic interactions between the two crystals after assuming Morse or Lennard-Jones potentials. Van der Merwe[28] considered an orientation-dependent contribution to the energy in a rigid overgrowth and substrate system by using a truncated Fourier series to express the interaction potential between the overgrowth and substrate atoms. Braun[30,31] generalized Van der Merwe's approach[28] into reciprocal space and derived an expression for the interaction energy, $V(x,y)$, between an individual interfacial overgrowth atom and the substrate surface in Fourier form as a function of atom positions:

$$V(x,y)=\sum_{\mathbf{q}} V_{\mathbf{q}}\exp(i\mathbf{q}\cdot\mathbf{r}_a) = \sum_{h,k} V_{hk}\exp[i2\pi(hx+ky)] , \quad (1)$$

where $\mathbf{r}_a=x\mathbf{a}_1+y\mathbf{a}_2=\mathbf{r}_{xy}$ represents the position of substrate surface atoms ($\mathbf{a}_1$ and $\mathbf{a}_2$ are basis vectors of the substrate surface unit cell), $\mathbf{q}=h\mathbf{a}_1^*+k\mathbf{a}_2^*=\mathbf{q}_{hk}$ is a lattice vector of the substrate surface reciprocal lattice (defined by $\mathbf{a}_i\cdot\mathbf{a}_j^*=2\pi\delta_{ij}$, $i,j=1,2$), and x, y, h, and k are integers. $V_{\mathbf{q}}$ or V_{hk} are Fourier coefficients appropriate to the two equivalent forms of the series and are chosen to ensure that the minimum of the potential is zero, allowing the direct interpretation of the interaction potential as misfit energy.

For the overgrowth it is assumed that there are $(2M+1)$ rows and $(2N+1)$ columns of lattice points, and these points are displaced by the vectors $\mathbf{r}_b=m\mathbf{b}_1+n\mathbf{b}_2=\mathbf{r}_{mn}$ with m from $-M$ to $+M$ and n from $-N$ to $+N$ ($\mathbf{b}_1$ and $\mathbf{b}_2$ are basis vectors of the overgrowth surface unit cell, while $\mathbf{b}_1^*$ and $\mathbf{b}_2^*$ with $\mathbf{b}_i\cdot\mathbf{b}_j^*=2\pi\delta_{ij}$ define the overgrowth surface reciprocal lattice). As M and N approach infinity, the overgrowth becomes a complete monolayer. If each of the overgrowth atoms lies at a minimum of the energy in the substrate potential as expressed in Eq. (1), the total interaction energy obtained by summing the individual contributions of each atom will be zero. Any deviation from this exact matching situation (misfit then exists) yields an energy greater than zero, which is interpreted directly as misfit energy.

After summing individual energy contributions over all the atoms in the overgrowth, the total interaction energy, or the misfit energy, between the overgrowth and substrate is

$$V=\sum_{h,k} V_{hk}F_{hk}F_{pq}[\sin\pi(2M+1)p(h,k)/\sin\pi p(h,k)] \times[\sin\pi(2N+1)q(h,k)/\sin\pi q(h,k)] , \quad (2)$$

where F_{hk} and F_{pq} are structure factors arising from the specific atomic arrangement in the substrate and overgrowth unit cells (that is, when non-Bravais lattices are used), and $p(h,k)$ and $q(h,k)$ are the components of the substrate reciprocal-lattice vector $\mathbf{q}_{hk}$, expressed in the overgrowth reciprocal lattice.

Direct calculation of Eq. (2) shows that the interaction energy, or the misfit energy, will be sharply minimized when p and q are integers. This means that a translational vector of the substrate reciprocal lattice, $\mathbf{q}_{hk}$, must coincide with a translational vector of the overgrowth reciprocal lattice, $\mathbf{q}^{pq}$, to yield a minimum interfacial misfit energy. That is,

$$\mathbf{q}_{hk}=\mathbf{q}^{pq} . \quad (3)$$

This essentially defines a necessary geometric yet general condition for an ideal epitaxial configuration. At equilibrium, systems with such an orientation and associated ratio of lattice constants as defined in Eq. (3) will be found to yield the lowest interfacial energy and are, therefore, favorable for epitaxy. This epitaxial criterion can be extended to two-dimensional matching, and in such cases it is required that Eq. (3) be satisfied by two noncolinear pairs of substrate and overgrowth reciprocal-lattice vectors.

For real systems with dissimilar lattice constants, there are both orientational and dimensional mismatches existing at the interface between the two crystals. These mismatches can be accommodated in several ways. If the thin overgrowth is allowed to strain homogeneously to satisfy Eq. (3), the misfit energy will be minimized but at the cost of increasing strain energy, both of which contribute to the interfacial energy. The strain energy can be calculated directly from the strain and known plane stress elastic constants (suitable for thin films) for any particular overgrowth orientations. Alternatively, misfit dislocations may be introduced to accommodate the misfit and strain, thereby reducing the interfacial energy. Pure edge dislocations are used to compensate the dimensional misfit, whereas pure screw arrays are used to accommodate the orientational misfit. The dislocation structures, including Burgers vectors, spacings, and orientation of dislocation arrays can be calculated in any

given interfacial orientation with a single formulation. The misfit dislocations have actually been observed at the diamond/β-SiC interface and will be discussed in more detail later.

In addition, the epitaxial criterion discussed above has been qualitatively assessed to give an indication of the "tendency to yield epitaxy." A number of quality factors have been defined to rank various possible configurations which satisfy the epitaxial condition as expressed by Eq. (3). These factors include the following: (i) The relative density of coinciding reciprocal lattice points. Since lower interfacial energy will follow from more resonating terms as expressed in Eq. (2), it is desirable for an optimum configuration to have a high relative density of coinciding reciprocal-lattice points. (ii) The length of the coinciding reciprocal-lattice vectors. As the magnitude of Fourier coefficients tends to decrease rapidly with the order $|h|+|k|$ or $|p|+|q|$, the shorter resonating reciprocal-lattice vectors will make it more likely for the actual occurrence of the particular epitaxial configuration. (iii) The strain energy density. Because real systems are expected to strain to achieve pseudomorphic structure as required by Eq. (3), configurations with lower strain energy densities are preferred. These geometric factors will make it possible when selecting and ordering candidate systems for epitaxial growth to use the geometric criterion established by Eq. (3) in a simple and effective manner.

The searching method for possible epitaxial configurations obtained from Eq. (3) is implemented in an interactive computer program called ORPHEUS, written by Braun.[31] Briefly, the program produces scaled plots of the substrate and overgrowth reciprocal lattices (shown in Fig. 1) and interactively leads the user to a visualization in reciprocal space analogous to the Ewald sphere construction used in crystallography.[32] By selecting a substrate reciprocal vector $\mathbf{q}_{hk}$ and rotating it 360° about the origin, a circle is constructed. Any overgrowth point lying on this circle describes an overgrowth reciprocal-lattice vector $\mathbf{q}^{pq}$ equal in length to $\mathbf{q}_{hk}$. The angle between $\mathbf{q}^{pq}$ and $\mathbf{q}_{hk}$ determines the angle through which the overgrowth must be rotated to come into epitaxial orientation with the substrate. The strain needed to bring a vector nearly on the circle into coincidence and the associated energy is calculated from the components of the selected vectors. Plots showing the subsequent reciprocal lattices in coincidence are produced by the program, from which quality judgments of the density of points which coincide may be made. The reciprocal-lattice vectors thus uniquely define the matching atomic rows and their orientations.

The reliability of the geometric considerations depends strongly on the assumptions of the underlying model. Virtually the only input into the model is the symmetries of the planes forming the interface. No assumptions were made of the actual values of the Fourier coefficients, which means that no specific atomic interactions were assumed. The general nature of the criterion as a necessary condition for an epitaxial orientation derives from the absence of such specific assumptions. A further strength of the reciprocal space criterion lies in that it has been derived from two totally independent models, that is, an atomistic (three-dimensional) model using central potentials by Fletcher and Lodge[25,26] and the model described here which is based almost entirely on the symmetric properties of the interfacial atomic planes. However, apart from approximations inherent in the minimum-energy principle and the abrupt interface transition, several other simplifications reduce the predictive potential of these geometric considerations. While the Fourier coefficients may be calibrated by empirical data such as sublimation and surface energies, surface migration ener-

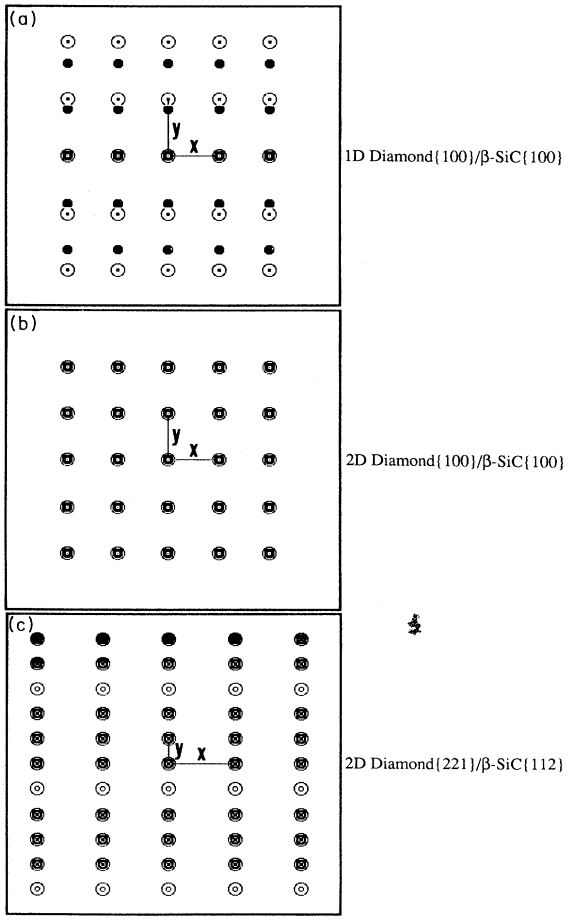

FIG. 1. Examples of superimposed reciprocal spaces of diamond and β-SiC planes after strain generated from the ORPHEUS computer program. (a) One-dimensional partial match between diamond {100} and β-SiC {100} after considering Poisson effect (strain: $\varepsilon_{xx}=22.2\%$, $\varepsilon_{yy}=-0.2\%$, $\gamma_{xy}=0$). (b) Two-dimensional pseudomorphic match between diamond {100} and β-SiC {100} (2D 100%, pair no. 1 in Table I) after isotropic strain of 22.2%. (c) Two-dimensional partial match between diamond {221} and β-SiC {112} ($O\%/S\%=73/100\%$, pair no. 1 in Table II) after strain of $\varepsilon_{xx}=22.2\%$, $\varepsilon_{yy}=-0.2\%$, and $\gamma_{xy}=0$. The symbols: ●, reciprocal-lattice points of substrate (β-SiC); ○, reciprocal-lattice points of overgrowth (diamond); ⊙, matched substrate and overgrowth points.

gies, and shear constants, the geometric considerations reported here did not involve any of these calibrations. Ideally, the theory only applies to a monolayer overgrowth, but the elastic and structural properties of the monolayer overgrowth are assumed to be the same as those of the bulk. In addition, the theory does not consider the nature of chemical bonding between the two crystals and possible interdiffusion, chemical reactions, or islanding at the interface as well as growth rate and temperature effects. Therefore, the criterion can only be used as a first tool, never the only and definitely not the last, in analyzing interfacial configurations and qualitatively explaining the behavior of epitaxial systems.

Despite the limitations, this geometrical model has been applied to many heteroepitaxial systems with different crystal symmetries and mismatches, and it has been found that such a description of the geometry of an epitaxial interface in reciprocal space is a useful tool for evaluating candidate interfacial configurations for epitaxy.[33–36] Most interestingly, this method has been used by Braun *et al.*[37] to study the diamond/cBN heteroepitaxial system. The calculation results indicate that heteroepitaxy of low-index-like planes between diamond and cBN has the greatest potential in minimizing interfacial energy. The configuration of diamond{100}/cBN {221} is next in potential, and all other matching configurations are less favorable. These geometric considerations correlated well with published experimental results.

III. RESULTS

A. Modeling

The theoretical analysis in this paper is mainly concerned with the selection of ideal epitaxial configurations between diamond and β-SiC. To apply the geometric method described above to the diamond/β-SiC system, primitive surface lattices were used for both diamond and β-SiC to avoid complications with structure factors due to nonprimitive unit-cell constructions. To construct the reciprocal spaces of both the diamond overgrowth and β-SiC substrate lattices, surface unit-cell parameters (angles and lengths of surface cell basis vectors) need to be known, and the relative lattice scaling parameter, which is usually given as the ratio of unstrained nearest-neighbor distances (NND), needs to be determined. A program called LATUSE/SARCH, developed by Hermann of Havelmatensteig 21, Berlin, Germany and Van Hove of Department of Chemistry at University of California at Berkeley, was used to determine the surface-cell structures. As both diamond and β-SiC share the geometry of zinc-blende structure, one set of unit-cell descriptions is sufficient for the low-index planes of both crystals which were considered. The ratio of unstrained nearest-neighbor distances for the lattices of diamond and β-SiC was determined to be 0.828 159 9. To calculate the strains and strain energy densities, two-dimensional plane stress elastic constants suitable to the overgrowth orientation are required. An ELCON program written by Braun[31] was used to transform bulk elastic constants to the required plane and to apply the plane stress boundary conditions as well. As stated earlier, the reciprocal space searches for ideal interfacial configurations were carried out with an interactive version of the program ORPHEUS.

The results are summarized in Tables I and II. A total of seven low index planes, {100}, {110}, {111}, {120}, {112}, {114}, and {221}, were considered as possible planes that each crystal may present at the interface. The two-dimensional matching conditions in reciprocal space of all the possible pairs of low-index-like planes and mixed planes of diamond and β-SiC as well as various orientations in any single plane pair were examined. In addition, the mixed pair of the {100} low-index plane of β-SiC and the {16,1,1} high-index plane of diamond, which was suspected to be a possible interfacial match observed in experiments (see discussion), was also studied. Results of calculated strain and strain energy densities are presented in the tables for selected matching pairs. The two-dimensional matching (parallel) directions and matching types as well as misfit dislocation densities in one of the matching directions are also indicated in the tables.

Table I presents selected pairs of two-dimensional (2D) pseudomorphic matches (designated as 2D 100% in the table) in reciprocal space with zero misfit energy and strain energy density less than 10^{12} erg cm^{-3}. It can be seen that a two-dimensional pseudomorphic match for like planes as shown in Fig. 1(b) requires an extensive isotropic strain of 22.2% with a strain energy density of about 6.0×10^{11} erg cm^{-3}. The small variations in strain energy densities among the various pairs of like planes are due to anisotropy of the elastic properties. In order to release the strain, misfit dislocations must be introduced at the interface at a relatively high density. The dislocation spacings in the second matching direction as indicated in the table range from 5 to 23 in units of effective (strained) nearest-neighbor distance in diamond, assuming all of the strain is released. However, for the unlike pair of diamond {114} and β-SiC {221} (pair no. 8 in the table), the two-dimensional pseudomorphic configuration results in a strain energy density of only 3.9×10^{11} erg cm^{-3}, which is nearly half of those for the like pairs. The density of misfit dislocations needed to release the strain energy is also much lower with a wider dislocation spacing of 28 NND in diamond. No other configurations listed in the table can compete with this pair on this energy level and dislocation density. Therefore, the pair of diamond {114} and β-SiC {221} appears to be a very promising configuration for diamond heteroepitaxy on β-SiC substrate.

Table I also presents the pair of the low-index plane of β-SiC {100} and the high-index plane of diamond {16,1,1}. This combination was examined because it possibly represents an orientational relationship at the interface between diamond and β-SiC observed in experiments, as discussed in the following sections. However, such a combination results in an extremely high strain energy density, which makes it unlikely to actually occur. Of other unlike pairs which could produce pseudomorphic two-dimensional matches but are not listed here, considerable strain energies in the range of $11.4-1495\times10^{11}$

TABLE I. Interfacial pairs of low-index planes with two-dimensional pseudomorphic matches in reciprocal space for the diamond and β-SiC heteroepitaxial system.

Pairs	Planes β-SiC	Planes Diamond	Parallel rows β-SiC‖Diamond	Strains ε_{xx} (%)[a]	Strains ε_{yy} (%)[b]	Strains γ_{xy} (%)[c]	Strain energy density ($\times 10^{11}$ erg cm^{-3})	Matching type	Spacing of misfit dislocations (unit of NND)
1	{100}	{100}	$[0\bar{1}1]\|\|[0\bar{1}1]$						
			$[0\bar{1}\,\bar{1}]\|\|[0\bar{1}\,\bar{1}]$	22.2	22.2	0	5.8	2D 100%	5.4
2	{110}	{110}	$[001]\|\|[001]$						
			$[1\bar{1}0]\|\|[1\bar{1}0]$	22.2	22.2	0	6.1	2D 100%	6.8
3	{111}	{111}	$[\bar{1}01]\|\|[\bar{1}01]$						
			$[1\bar{1}0]\|\|[1\bar{1}0]$	22.2	22.2	0	6.2	2D 100%	5.0
4	{120}	{120}	$[2\bar{1}1]\|\|[2\bar{1}1]$						
			$[00\bar{1}]\|\|[00\bar{1}]$	22.2	22.2	0	6.0	2D 100%	8.9
5	{112}	{112}	$[\bar{1}\,\bar{1}1]\|\|[\bar{1}\,\bar{1}1]$						
			$[1\bar{1}0]\|\|[1\bar{1}0]$	22.2	22.2	0	6.1	2D 100%	12.8
6	{114}	{114}	$[\bar{2}\,\bar{2}1]\|\|[\bar{2}\,\bar{2}1]$						
			$[1\bar{1}0]\|\|[1\bar{1}0]$	22.2	22.2	0	5.9	2D 100%	22.8
7	{221}	{221}	$[\bar{1}\,\bar{1}4]\|\|[\bar{1}\,\bar{1}4]$						
			$[1\bar{1}0]\|\|[1\bar{1}0]$	22.2	22.2	0	6.2	2D 100%	14.6
8	{221}	{114}	$[\bar{1}\,\bar{1}4]\|\|[\bar{2}\,\bar{2}1]$						
			$[1\bar{1}0]\|\|[1\bar{1}0]$	22.2	−13.6	0	3.9	2D 100%	27.8
9	{100}	{120}	$[0\bar{1}1]\|\|[2\bar{1}1]$						
			$[0\bar{1}\,\bar{1}]\|\|[00\bar{1}]$	−15.9	−15.9	−19.9	7.6	2D 100%	2.7
10	{111}	{120}	$[\bar{1}01]\|\|[2\bar{1}1]$						
			$[1\bar{1}0]\|\|[00\bar{1}]$	−13.6	−33.1	0	7.7	2D 100%	3.4
11	{100}	{16,1,1}	$[0\bar{1}1]\|\|[1\bar{8}\,\bar{8}]$						
			$[0\bar{1}\,\bar{1}]\|\|[01\bar{1}]$	22.2	−92.4	0	45.7	2D 100%	1.3

[a] ε_{xx} is the normal tensile strain in the x direction (designated in Fig. 1).
[b] ε_{yy} is the normal tensile strain in the y direction (designated in Fig. 1).
[c] γ_{xy} is the shear strain on a plane whose normal is in the x direction but in a direction coincident with the y direction.

TABLE II. Interfacial pairs with two-dimensional partial matching in reciprocal space for the diamond and β-SiC heteroepitaxial system.

Pairs	Planes β-SiC	Planes Diamond	Parallel rows β-SiC‖Diamond	Strains ε_{xx} (%)[a]	Strains ε_{yy} (%)[b]	Strains γ_{xy} (%)[c]	Strain energy density ($\times 10^{11}$ erg cm^{-3})	Matched lattice points ($O\%/S\%$)
1	{112}	{221}	$[\bar{1}\,\bar{3}2]\|\|[0\bar{1}2]$					
			$[1\bar{1}0]\|\|[1\bar{1}0]$	22.2	−0.2	0	2.9	73/100
2	{221}	{120}	$[\bar{1}02]\|\|[2\bar{1}1]$					
			$[1\bar{1}0]\|\|[00\bar{1}]$	−13.6	16.0	0	2.2	100/51
3	{114}	{120}	$[1\bar{1}0]\|\|[00\bar{1}]$					
			$[\bar{3}11]\|\|[2\bar{1}1]$	−13.8	9.9	5.7	1.8	100/33
4	{112}	{120}	$[\bar{1}\,\bar{3}2]\|\|[2\bar{1}\,\bar{1}]$					
			$[1\bar{1}0]\|\|[00\bar{1}]$	−13.6	−5.3	0	1.2	78/53
5	{100}	{120}	$[0\bar{1}1]\|\|[2\bar{1}1]$					
			$[0\bar{1}\,\bar{1}]\|\|[2\bar{1}\,\bar{5}]$	−3.5	4.0	4.1	0.3	29/60
6	{111}	{221}	$[0\bar{1}1]\|\|[\bar{1}\,\bar{1}4]$					
			$[2\bar{1}\,\bar{1}]\|\|[1\bar{1}0]$	5.9	1.9	0	0.2	22/49
7	{110}	{110}	$[001]\|\|[\bar{1}12]$	32.4	14.1	−24.4	14.9	24/24
			$[1\bar{1}0]\|\|[1\bar{1}0]$	15.2	44.0	−40.7	31.7	70/76

[a] ε_{xx} is the normal tensile strain in the x direction (designated in Fig. 1).
[b] ε_{yy} is the normal tensile strain in the y direction (designated in Fig. 1).
[c] γ_{xy} is the shear strain on a plane whose normal is in the x direction but in a direction coincident with the y direction.

erg cm^{-3} were calculated, which make them compare unfavorably with the pairs listed in the table.

Table II lists selected pairs of two-dimensional partial or coincidental matches in reciprocal space which yield lower strain energies but at the cost of increased misfit energies. In these cases, some substrate vectors do not have counterparts in the overgrowth reciprocal lattice or vice versa, which results in high-order coincidence matches, as shown in Fig. 1(c). The partially matched pairs form a hierarchy in Table II ordered by the densities (or percentages) of reciprocal-lattice points that are paired in both the overgrowth and substrate, denoted by $O\%$ and $S\%$, respectively. Since both the strain and misfit energies contribute to the overall interfacial energy, which governs whether a heteroepitaxial interface will form, the actual occurrence of such a partially matched configuration will depend on the gain of strain energy versus the loss of misfit energy. Empirically speaking, below the critical thickness,[24] these partially matched pairs are, in general, not expected to compete with the pseudomorphic pairs listed in Table I because of the zero misfit energy of the latter. However, only specific growth conditions will dictate which configuration will actually occur, and factors such as surface energies and growth kinetics will play important roles in determining which configuration is more favorable for epitaxy in reality.

Included in Table II are also the like pair of diamond {110} and β-SiC {110} with one-dimensional diamond ⟨112⟩ parallel to β-SiC ⟨100⟩, which is reported to be a favorable orientation for epitaxy.[38] However, the examination by the current model suggests that the matching is poor and the strain is high for this particular one-dimensional matching case. For two-dimensional matches, the strain energy is even higher, while the matching density remains unsatisfactory. Therefore, the configuration appears unfavorable compared to the many pairs listed in Table I.

B. Experiments

The heteroepitaxial growth of diamond on β-SiC was conducted in an ASTeX stainless-steel microwave plasma CVD (MPCVD) reactor. The details of the MPCVD system have been described elsewhere.[39,40] Diamond was deposited on a 1-in-diam (001)-oriented β-SiC film which was grown epitaxially in a separate reactor on a (001) Si substrate using thermal CVD techniques.[19,41] The β-SiC film (4–5 μm thick) was prepared by polishing the as-grown surface with 0.1-μm diamond paste to minimize the surface roughness. The sample was then oxidized in O_2 at 1200 °C to a thickness of approximately 0.1 μm in order to remove the majority of the surface damage that occurred during the polishing. The oxidation was also expected to eliminate all the possible carbon and hydrocarbon contaminations which may have occurred during polishing. Immediately prior to insertion into the growth chamber, the oxide was stripped using a 10:1 mixture of HF:DI-H_2O followed by a DI-H_2O rinse and drying with nitrogen.

Prior to the diamond growth, the β-SiC substrate was pretreated using an *in situ* dc biasing technique to enhance the diamond nucleation density. This technique has been described in detail in earlier publications.[39,40] Briefly, the pretreatment consisted of biasing the substrate for 30 min at negative 250 V while it was immersed in a 4.0% methane-in-hydrogen plasma. The microwave power input was 600 W, the pressure was 15 torr, and the total gas flow rate was 1000 standard cubic centimeter per minute (SCCM). The resulting biasing current was 100–150 mA over a 2-in-diam molybdenum substrate holder. The substrate temperature was approximately 650 °C. After the 30-min pretreatment, the biasing voltage was turned off, and the substrate was moved to a position approximately 1 cm outside of the edge of the luminous plasma region. Simultaneously, the methane concentration was reduced to 1.0% in hydrogen, the pressure increased to 25 torr, and the substrate temperature was maintained at 650–700 °C. These growth conditions have in the past resulted in high-quality diamond films with little secondary nucleation and growth rates of about 0.05 μm/h. Diamond was grown on the (001) β-SiC substrate under the above conditions for 50 h. The sample was subsequently analyzed by scanning electron microscopy (SEM), cross-sectional transmission electron microscopy (XTEM), and Raman spectroscopy.

Figures 2(a) and 2(b) show SEM micrographs taken from both the center and edge of the sample, respectively. The arrow in Fig. 2(a) corresponds to the [110] direction of the β-SiC substrate. As seen from the schematic representation in Fig. 2(c), a high percentage of the diamond grains are aligned with the substrate with diamond {001} faces parallel to the β-SiC(001) face and diamond ⟨110⟩ directions parallel to the β-SiC [110] direction. It is also apparent that there is an azimuthal misorientation of several degrees among some of the diamond grains.

The epitaxial relationship between the diamond and β-SiC was confirmed by XTEM and transmission electron diffraction (TED). Figure 3 shows an XTEM micrograph of the diamond/(β-SiC) interface. The inset is the corresponding TED pattern with the electron beam incident along the β-SiC [110] direction. It can be seen from this diffraction pattern that two diamond {111} spots are rotated slightly about the β-SiC [110] axis relative to the β-SiC {111} spots, indicating the diamond overgrowth is tilted relative to the β-SiC substrate. A schematic of the TED pattern is shown in Fig. 4, from which this tilt angle is measured to be approximately 5°.

This tilt is even more evident when the interface is examined in high resolution, as shown in Fig. 5 and schematically in Fig. 6(a). In this [110] projection, the diamond $(1\bar{1}1)$ planes are shown to be continuous across the interface. However, there is a tilt of 4°–6° of the diamond $(1\bar{1}1)$ planes about the [110] axis towards the interfacial (001) plane. The large fringes near the interface are moiré fringes, indicating that there is a lattice overlapping between the diamond and β-SiC in this region. These moiré fringes are believed to be caused by the interfacial roughness.

There are also planar defects present which originate at the interface, as is evident from the dark contrasted bands fanning out from the interface, as shown in Figs. 3 and 5. In addition, there is an array of misfit dislocations

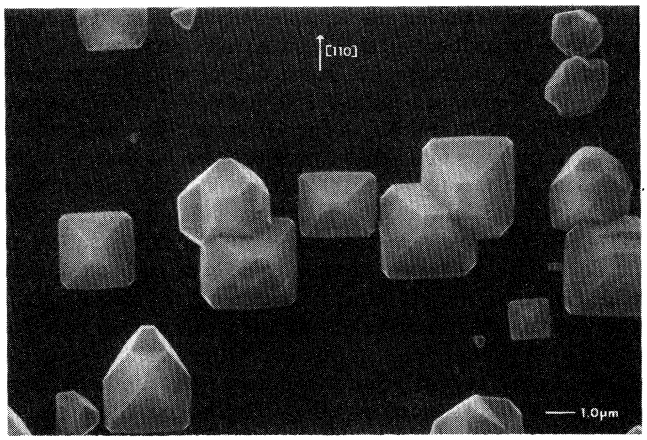

(a)

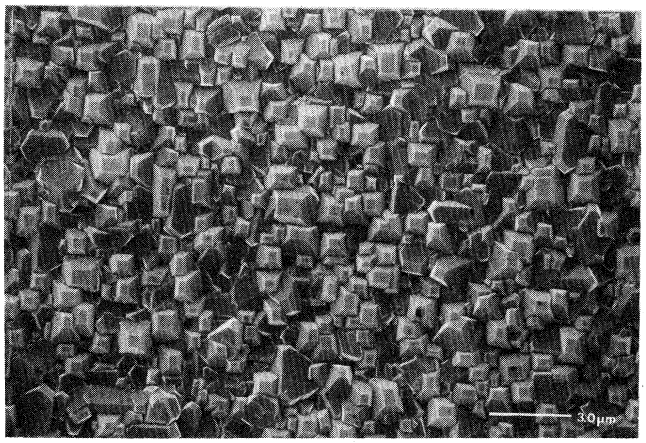

(b)

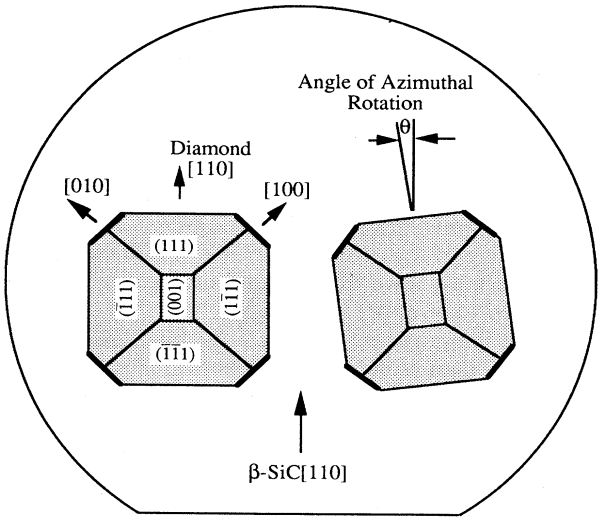

(c)

FIG. 2. SEM micrographs of textured diamond grains grown on β-SiC substrate taken from (a) the center and (b) the edge of the sample, and (c) is a schematic representation of the orientations of diamond grains with respect to the β-SiC substrate surface.

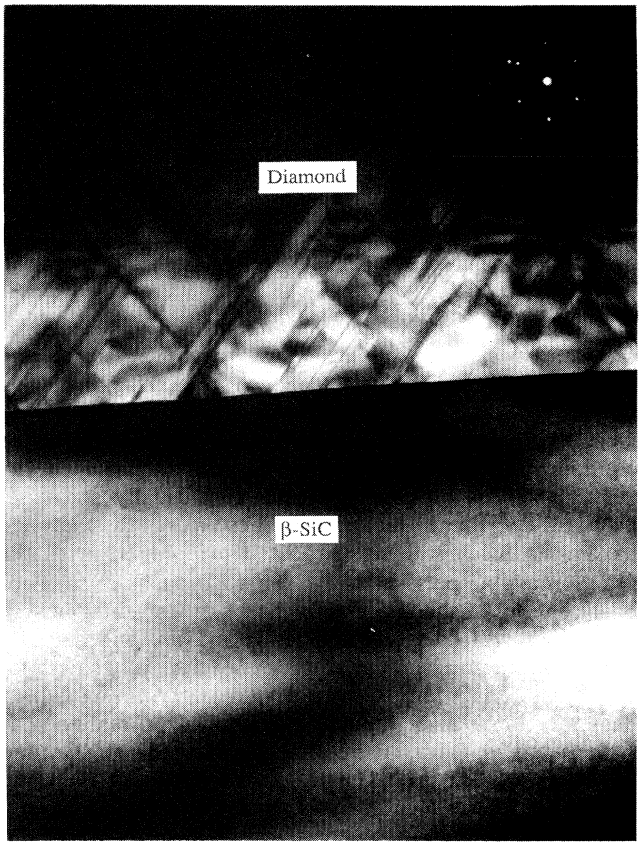

FIG. 3. An XTEM micrograph of the diamond/β-SiC interface and the corresponding TED pattern.

in diamond resulting from the large lattice mismatch at the interface (indicated by arrows in Fig. 5). The dislocation spacing can be measured as on average one misfit dislocation every seven lattice planes, which corresponds to a dislocation density (ρ) of 0.14 per lattice plane. This dislocation density is very close to the theoretical calcula-

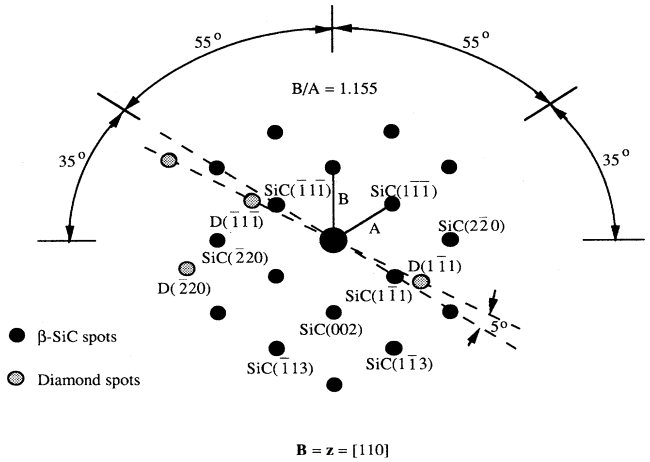

FIG. 4. A schematic, indexed diagram of the TED pattern shown in Fig. 3.

tion presented in Table I (one dislocation about every five lattice planes for pair no. 1), considering that the theoretical value assumes all the misfit strain is absorbed by pure edge-type dislocations, while in reality a portion of the strain may still remain at the interface. In addition, since the dislocations in diamond are commonly of the 60° mixed type,[42] they not only accommodate the misfit strain but also are responsible for the interfacial tilt and azimuthal rotation, as will be discussed in detail in the next section.

It is also important to note that there does not appear to be an interfacial layer between the diamond and β-SiC. In a previous study of bias-enhanced diamond nucleation on silicon,[40] it was found that the biasing process could effectively remove the surface oxide, and an amorphous interfacial layer containing both carbide and nondiamond carbon was observed. In that particular study, the biasing pretreatment lasted for 1 h, while here it was performed only for 30 min. By reducing the pretreatment time, it is believed that nucleation was still enhanced sufficiently over that for an untreated surface via the impingement of carbon-containing ions from the plasma; however, the surface damage and the formation of an amorphous layer were minimized, which, in conjunction with the oxide removal, allowed the heteroepitaxial nucleation and growth of diamond on β-SiC.

IV. DISCUSSION

Before embarking on a detailed discussion on the interfacial properties of the diamond and β-SiC system, it is helpful to briefly examine the general energetic requirements for a two-dimensional heteroepitaxial system and thus to appreciate the approach taken in the present

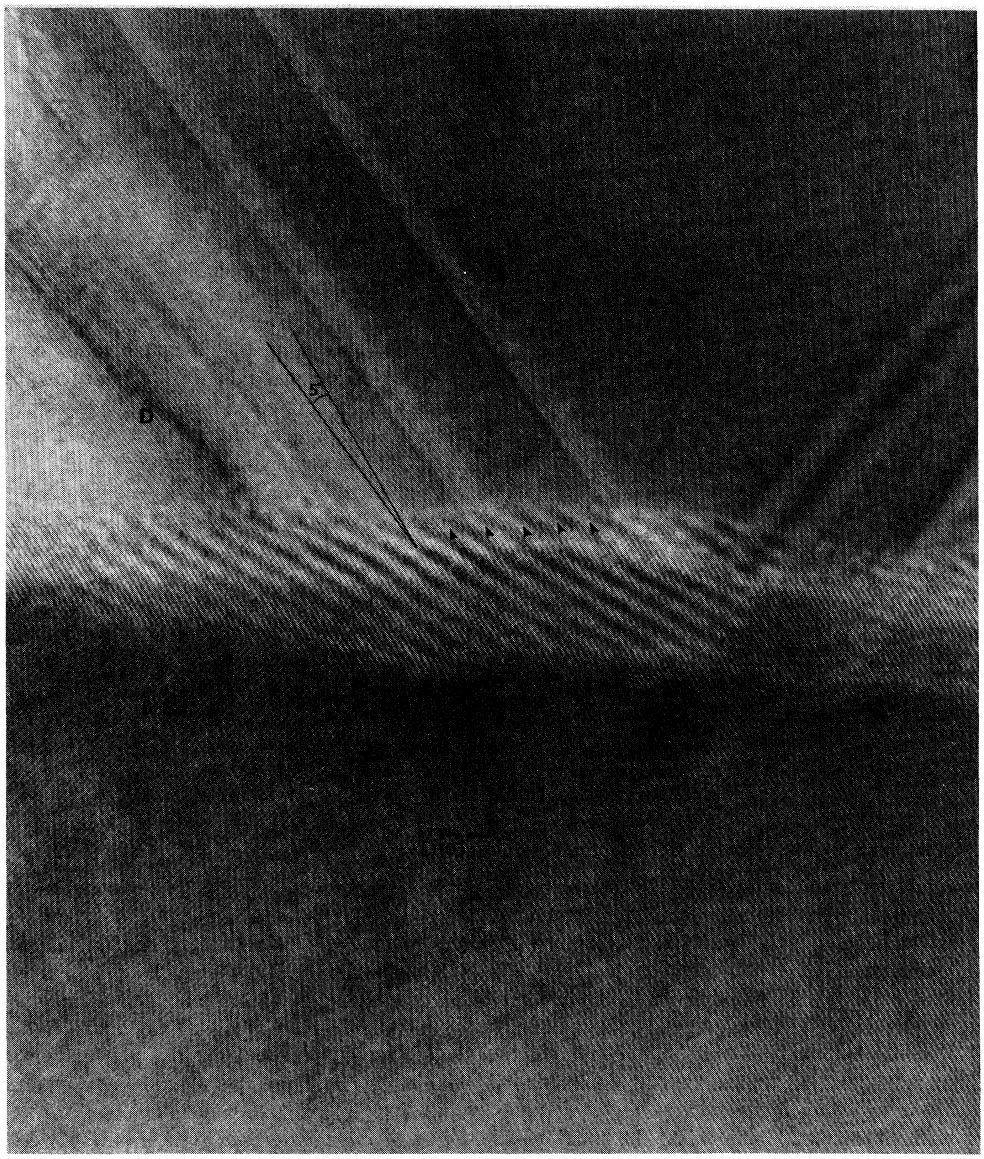

FIG. 5. A HRTEM micrograph of the diamond/β-SiC interface. Arrows indicate the positions of misfit dislocations.

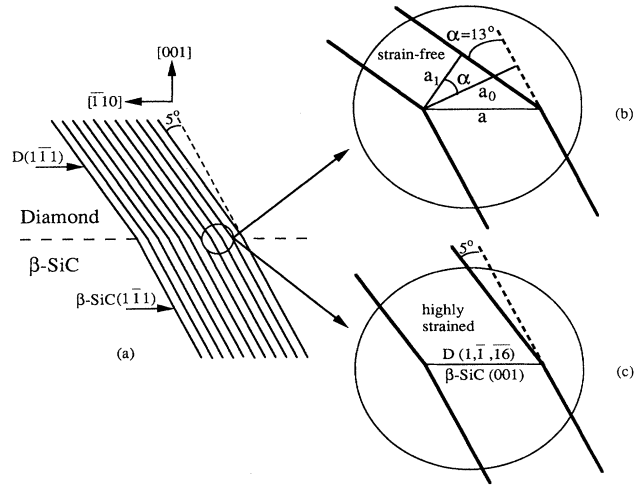

FIG. 6. Schematic diagrams of (a) the tilted interface shown in the HRTEM micrograph in Fig. 5, and (b) and (c) an unlikely mechanism responsible for the interfacial tilt involving the matching of a high-index plane of diamond with a low-index plane of β-SiC. (b) is a strain-free situation which requires a 13° tilt of the diamond lattice, and (c) is a highly strained case which exposes diamond $\{16,1,1\}$ planes at the interface.

study of minimizing the interfacial energy to achieve diamond heteroepitaxy. It is known that for a heteroepitaxial system, the following general condition must be met to form an epitaxial overgrowth with two-dimensional, layer-by-layer growth (the Frank–van der Merwe model[24]), assuming no chemical reactions or interdiffusion at the interface:

$$\sigma_s > \sigma_o + \sigma_{im} + \sigma_{is} , \tag{4}$$

where σ_s is the surface free energy (or surface energy) of the substrate, σ_o is the surface free energy (or surface energy) of the overgrowth, σ_{im} is the interfacial energy associated with the lattice mismatch, and σ_{is} is the interfacial energy related to the strains. If this inequality has the opposite sign, three-dimensional island growth (the Volmer-Weber[43] or Stranski-Krastanov[44] model) will occur. Therefore, for two-dimensional diamond growth to occur, the diamond surface energy (σ_o) and the interfacial misfit and strain energies (σ_{im} and σ_{is}) must be minimized or the substrate surface energy (σ_s) must be raised. Efforts in reducing the high surface energy of diamond by using surfactants and increasing the surface energy of the substrate by roughening and/or introducing high concentrations of surface defects have been attempted.[45] However, two-dimensional diamond heteroepitaxy has not yet been observed.

Obviously, in addition to maximizing the substrate surface energy and minimizing the diamond surface energy to satisfy Eq. (4), it is necessary to reduce the interfacial energy by minimizing the interfacial misfit and strain. This requires any nondiamond substrates to be closely lattice matched with diamond. Otherwise, the high misfit and strain energies will cause immediate island nucleation and growth, even if the surface energy of diamond is lowered. Considering the nearly insurmountable high surface energy of diamond, this approach of minimizing the interfacial energy appears to be more feasible for two-dimensional diamond heteroepitaxy. There has been significant experimental evidence indicating that the interfacial structure and associated energy play important roles in the formation of diamond on foreign substrates. For example, it is reported that diamond nucleates more easily on carbide-forming substrates (Mo, W, Si, Ta, Nb) than on non-carbide-forming substrates (Cu, Pt, Au) (see Ref. 46 and references cited therein), suggesting that the formation of interfacial carbide layers may lower the interfacial energy between diamond and the substrates, and thus promote the diamond nucleation.

The theoretical model employed in this paper addresses the contributions to the interfacial misfit and strain energies by geometric factors such as the orientation and surface unit-cell periodicity of each interfacial plane. The model is based on Van der Merwe's row matching epitaxial criterion,[28] namely, that an ideal configuration is equivalent to the matching of a certain set of consecutive atomic rows in the overlayer with a parallel set in the substrate. It incorporates various modes to accommodate the misfit, including simple rotation, homogeneous strain, and misfit dislocations. By considering the energy due to lattice mismatch, a geometric criterion is derived which is conveniently formulated in the reciprocal lattices of two crystal surface systems, and various measures of quality are established to correlate with the achievement of epitaxy. By calculating the orientational and dimensional misfits, the misfit strain and dislocation structures, it predicts ideal configurations on energetic grounds and allows for analytical selection of ideal epitaxial configurations of any heteroepitaxial systems.

The modeling results indicate that the match of low-index-like planes between diamond and β-SiC requires extensive strain to reach two-dimensional pseudomorphic configurations. This is not surprising, considering the substantial lattice constant mismatch of 18% between diamond and β-SiC. The resulting strain energy densities for the like pairs reach 10^{11} erg cm^{-3}, which is two orders of magnitude higher than those for the like pairs in the diamond/cBN system. Therefore, unlike other better lattice-parameter matched heteroepitaxial systems such as diamond/cBN (1.3%), Ge_xSi_{1-x}/Si (0–4.2 %), GaP/Si (0.4%), AlP/Si (0.6%), ZnS/Si (0.4%), and GaAs/Si (4.1%), where like plane epitaxy commonly occurs,[1,3,47–49] the like pairs in the diamond/β-SiC system are energetically less favorable for epitaxy unless some of the strain can be relieved by various possible mechanisms. This strain release is realized in the present diamond/β-SiC system by the introduction of misfit dislocations, which has been observed experimentally. The generation of misfit dislocations to accommodate the strain is a very common phenomenon in many lattice-mismatched heteroepitaxial structures such as Si/GaP,[42] GaAs/Si,[50,51] and GaAsP/GaAs.[52] The dislocations occur when the energy associated with the strain exceeds that to be gained by matching. This is particularly true when the overgrowth reaches a certain thickness, since

the onset of dislocation normally occurs at a critical thickness.[24,53,54] Energy is lowered as a consequence of the elastic relaxation associated with the misfit dislocations. Under such conditions, any strain will be localized, and the reciprocal vectors will not coincide completely. These dislocations not only reduce the strain and thus enhance the tendency to epitaxy, but also modify the interfacial structure, which may directly affect the properties. Understanding and controlling these dislocations is thus of great importance.

For the diamond and β-SiC interface, it was shown in Figs. 5 and 6(a) that a tilt boundary developed. A misorientation of this nature is not desirable, since it results in low-angle grain boundaries among the various diamond grains once they grow into a complete film. A high density of low-angle grain boundaries can be expected to degrade the electrical properties of the resulting film. The possible mechanisms responsible for the tilt include (i) a high index plane exposed by the diamond overgrowth to match the low index plane of β-SiC substrate, thus reducing the lattice mismatch and the resulting strain energy, and (ii) an array of misfit dislocations at the interface, which results in the tilt, similar to the classic structural model of a low-angle grain boundary.[55] It will be shown in the following discussion that the first mechanism is unlikely to occur, whereas the second mechanism is a reasonable explanation of the tilt phenomenon.

The first mechanism is shown schematically in Figs. 6(b) and 6(c). The amount of mismatch between the two dissimilar lattices may be reduced by tilting the smaller lattice to expose a higher index plane to the interface. As shown, the β-SiC and diamond have {111} lattice spacings of a_0 and a_1, respectively. By tilting through an angle α, the lattice spacing of the smaller lattice (diamond) may be made to match that of the larger one (β-SiC) in this simple one-dimensional model [see Fig. 6(b)]. When all of the mismatch is accounted for by this tilt, resulting in a one-dimensional pseudomorphy without strain, the tilt angle may be calculated from simple geometry as

$$\alpha = \cos^{-1}(a_1/a) - \cos^{-1}(a_0/a) , \quad (5)$$

where $a_1 = 3.57/\sqrt{3}$, $a_0 = 4.36/\sqrt{3}$, and a is the lattice spacing of the β-SiC($1\bar{1}1$) planes along the $[\bar{1}10]$ direction which equals $4.36/\sqrt{2}$. Substituting these values into Eq. (5), this one-dimensional rotation angle would be $\alpha = 13°$. However, the tilt observed in the HRTEM micrograph was approximately 5°, which only offsets a lattice mismatch of about 30%. Furthermore, the high index plane of diamond exposed by the 5° tilt is close to the {16,1,1} [see Fig. 16(c)]. Utilizing the theoretical model, the calculation suggests that the strain energy is very high when the diamond {16,1,1} is matched with the β-SiC {100} (see pair no. 11 in Table I). It is, therefore, unlikely that the observed tilt is a result of this type of mechanism involving the match of a high index plane of diamond with a low index plane of β-SiC.

The second possibility is that the tilt may be caused by the large number of misfit dislocations existing at the interface. If this is the case, the epitaxial relation should still be diamond (001) oriented with β-SiC(001). It is well known that the misfit dislocations in diamond lattices consist mostly of the 60° mixed type.[42,56,57] These 60°-type dislocations may be resolved into several components relative to a (001) interface, as discussed by Olsen and Ettenberg.[58] These include tilt (b_1), misfit (b_2), and azimuthal rotation (b_3) components, as schematically shown in Fig. 7. The misfit component (b_2) accommodates the strain via relaxation of the lattice through the formation of a misfit dislocation, whereas the tilt and azimuthal rotation components (b_1 and b_3) cause the diamond grains to rotate about the [110] and [001] axes, respectively. Both the tilt (b_1) and misfit (b_2) components are pure edge-type dislocations, while the azimuthal rotation component (b_3) involves a pure screw-type dislocation. Figure 8 indicates how a tilt boundary may develop from an array of edge-type dislocations running parallel to the interface.[55] The magnitude of the tilt resulting from an array of pure edge-type dislocations may be calculated from the relationship[59]

$$\sin\alpha = |b|/D , \quad (6)$$

where b is the Burgers vector, and D is the dislocation spacing.

In a (001)-oriented diamond lattice, a 60° mixed-type dislocation along a [110] direction on a $(1\bar{1}1)$ plane will have a Burgers vector, $b = a/2[011]$ (a is the lattice parameter of diamond), inclined 45° to the interface.[58] The tilt component (b_1) of this Burgers vector will be in the [001] direction with $b_1 = 0.707b$. Therefore, according to Eq. (6), the tilt angle may be calculated as

$$\sin\alpha = 0.707|b|/D . \quad (7)$$

Here, the quantity $|b|$ equals $a/\sqrt{2}$, and $1/D$ is simply the dislocation density. From Fig. 4, there is on average

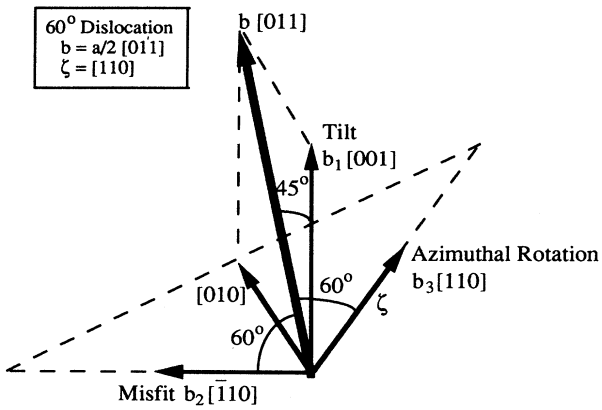

FIG. 7. The decomposition of a 60° dislocation in diamond into tilt (b_1), misfit (b_2), and azimuthal rotation (b_3) components.

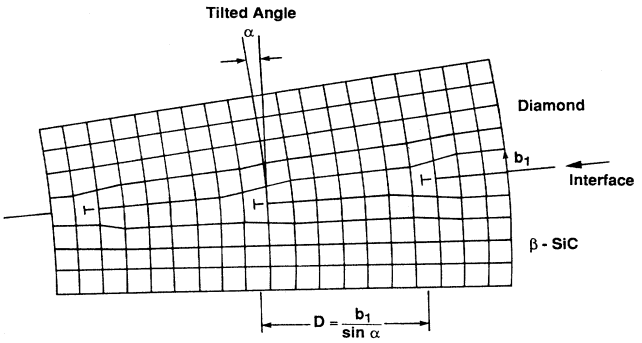

FIG. 8. A schematic diagram of a tilted interface caused by an array of edge-type dislocations parallel to the interface.

a dislocation density (ρ) of 0.14 per {111} lattice plane along the [$\bar{1}$10] direction. With this dislocation density, the tilt angle is $\alpha=\sin^{-1}[0.707(a/\sqrt{2})(\sqrt{2}/a)\rho]=6°$, which is in very good agreement with the measured angle of 5°. Therefore, it can be concluded that the high density of misfit dislocations is most likely responsible for the observed interfacial tilt. Using a similar approach but assuming a twist boundary model,[60] the angle of azimuthal rotation involving the screw component (b_3) can be calculated as $\theta=\sin^{-1}[0.5(a/\sqrt{2})(\sqrt{2}/a)\rho]=4°$, which is also in good agreement with the experimental observations.

It is interesting to point out that the measured misfit dislocation density is lower than that expected for a roughly 20% lattice mismatch between diamond and β-SiC. If all of the strain energy is absorbed by perfect edge-type misfit dislocations, one would expect on average one dislocation for every five lattice planes, or a dislocation density of 0.2 per lattice plane, as calculated by the model. However, for the 60°-type dislocations, the misfit component (b_2) will be along the interface in the [$\bar{1}$10] direction, with $b_2=0.5b$. Therefore, the mixed dislocations are only half as efficient in relieving the misfit strain as the perfect edge type. As a result, the predicted dislocation density should increase to 0.4 per lattice plane, or one dislocation every 2.5 lattice planes. This implies that the diamond overgrowth observed in this study is still strained near the interface. If the interfacial strain was minimized by a dislocation density of 0.4 per lattice plane, the predicted tilt angle, calculated via Eq. (7), would be approximately 16° instead of the observed 5°.

It can be seen from this discussion that an epitaxial configuration with lower interfacial strain (and thus fewer misfit dislocations) will have a greater potential in producing heteroepitaxial structures with smaller misorientations. In this regard, the system of diamond {114} with β-SiC {221} appears to be very promising. Not only is the misfit energy minimized to zero for pseudomorphic growth, but the cost of strain energy is only half of that for the diamond/β-SiC like-pair pseudomorphic systems. Based on the logic presented above, if the strain energy is to be minimized via the incorporation of misfit dislocations at the interface, the maximum tilt angle would be only approximately 8° versus 16° for the diamond {100}/β-SiC {100} case. If the interface is to remain partially strained, as observed by XTEM in the present study, then an interface with a tilt angle of less than 5° could be achieved. The epitaxy involving such mixed planes (often referred to as inclined or double-positioned epitaxy) is not uncommon in semiconductor heterostructures such as β-SiC(411)/Si(511) (Ref. 61) and CdTe(111)/GaAs(100),[62] as well as epitaxial metals and fluorides on semiconductors such as Al/GaAs and CaF_2/Si.[63,64] Such nonparallel orientations have typically shown smaller mismatches and reduced defects at the interface. Therefore, from the geometric considerations, experimental attempts of heteroepitaxial nucleation and growth of diamond on the β-SiC {221} plane are strongly recommended.

This model has established a system of essentially geometric selection criteria to order candidate epitaxial configurations by their potential to minimize interfacial energy and thus represents a general, geometric reciprocal space technique for evaluating candidates for epitaxial growth. It has its greatest value as a sieve or selector of candidate interfacial structures and provides useful detailed geometric insights about the epitaxial systems. However, it must be used with adequate caution. As indicated earlier, the energy calculations are solely based on geometric considerations, not taking into account the effect of surface chemical bonding on the interfacial energy. This may be a liability when considering that the β-SiC substrate could have either carbon or silicon terminated surfaces for certain planes. The different atomic terminations on the substrate surface are expected to have differing effects on the interfacial misfit energy when diamond is bonded to them. Also, the model is not applicable to interfaces which are composed of diffused or converted layers rather than a singular, atomically smooth plane such as those of β-SiC/Si, GeSi/Si and many III-V and II-VI structures.[20,65–68] In addition, the interfacial energy is not the only factor which influences the growth. The surface energy differences among the various planes may well play a role in determining the growth orientation and growth mode. For example, the diamond {111} orientation may have a better chance in promoting a two-dimensional layer growth mode because of its lower surface energy compared to the diamond {100} surfaces.

Furthermore, for interfacial pairs with partial or coincidence matches which are intermediate in terms of both misfit and strain energies, the model is unable to give a threshold of mismatch in interfacial configurations beyond which diamond will not grow epitaxially. Nor can the model supply an upper limit to the strain energy density above which diamond will not tolerate and maintain interfacial registry. While configurations in a particular pair of interfacial planes can be determined and ordered adequately by the geometric criterion, more detailed energetic, dynamic, and chemical bonding considerations are needed to adequately order coincidence configurations. In reality, the specific surface energy differences between the overgrowth and substrate and the kinetic factors such as growth rates in different crystallographic directions will play important roles in determin-

ing a configuration which will actually occur. For example, a reduced surface energy difference might allow less-favorable configurations, such as those listed in Table II, with poor lattice matches but less strain to actually occur. There are plenty of examples of successful growth of heteroepitaxial structures involving a triumph of kinetics over energetics by manipulating deposition temperatures and growth rates, as well as the use of surfactants.[13,69] Therefore, the careful manipulation of deposition parameters is certainly no less important than the selection of substrate materials and orientations. Since diamond heteroepitaxy is a complicated process which involves many issues other than the interfacial lattice mismatches, such as surface diffusion, clustering, chemical dissimilarity, etc., each and every stage in the heteroepitaxial growth process, from substrate surface preparation and cleaning to the post-growth cooling process, is of critical importance in determining the final epitaxial structure. Nevertheless, the model has given rise to a powerful technique for analyzing epitaxial systems. It is hoped that the resulting interfacial predictions will stimulate more meaningful experimental investigations and reliable theoretical analyses.

V. CONCLUSIONS

A theoretical examination of the diamond/β-SiC heteroepitaxial interface was performed utilizing a geometric criterion formulated in reciprocal space based on considerations of interfacial misfit and strain energies. The modeling results were compared with the experimental observations of the diamond/β-SiC interface. The calculations indicated that the unlike low index pair between diamond {114} and β-SiC {221} has the greatest potential in minimizing the interfacial energy and is, therefore, strongly recommended for experimental investigations. The low-index-like pairs between diamond and β-SiC are next in potential, and diamond (001)/β-SiC (001) heteroepitaxy has been confirmed via experimental observations. Other configurations yield high interfacial energies and are unlikely to occur in reality. The relatively high strain energy associated with the like-pair heteroepitaxy can be relieved by the introduction of misfit dislocations at the interface. These misfit dislocations have also been experimentally observed. The calculated misfit dislocation densities correlate well with the experimental measurements. The misfit dislocations observed in diamond not only accommodate the misfit strain but also cause both interfacial tilting and azimuthal rotational misorientations.

ACKNOWLEDGMENTS

The authors wish to thank Professor R. Davis and Mrs. Y. C. Wang for supplying the β-SiC single-crystal films for the present research. Financial support from Strategic Defense Initiative Organization/Innovative Science and Technology Branch through the Office of Naval Research and Kobe Steel, Ltd. is also gratefully acknowledged.

*Present address: Metal Industries Development Center, 1001 Kaonan Highway, Nantzu 81103, Kaohsiung, Taiwan.
†Present address: Cree Research Inc., 2810 Meridian Parkway, Durham, NC 27713.
‡Permanent address: Department of Physics, University of Pretoria, Pretoria 0002, South Africa.

[1]M. Yoshikawa, H. Ishida, A. Ishitani, T. Murakami, S. Koizumi, and T. Inuzuka, Appl. Phys. Lett. **57**, 428 (1990).
[2]M. Yoshikawa, H. Ishida, A. Ishitani, S. Koizumi, and T. Inuzuka, Appl. Phys. Lett. **58**, 1387 (1991).
[3]S. Koizumi, T. Murakami, T. Inuzuka, and K. Suzuki, Appl. Phys. Lett. **57**, 563 (1990).
[4]R. C. DeVries, *Cubic Boron Nitride: Handbook of Properties,* Report No. 72CRD178 (General Electric Company, Schenectady, NY, 1972).
[5]B. E. Williams and J. T. Glass, J. Mater. Res. **4**, 373 (1989).
[6]J. Narayan, A. R. Srivatsa, M. Peters, S. Yokota, and K. V. Ravi, Appl. Phys. Lett. **53**, 1823 (1988).
[7]D. G. Jeng, H. S. Tuan, R. F. Salat, and G. J. Fricano, Appl. Phys. Lett. **56**, 1968 (1990).
[8]Y. Sato, I. Yashima, H. Fujita, T. Ando, and M. Kamo, in *Proceedings of the Second International Conference on New Diamond Science and Technology,* edited by R. Messier, J. T. Glass, J. E. Butler, and R. Roy, MRS International Conference Proceedings (Materials Research Society, Pittsburgh, 1991), p. 371.
[9]B. V. Spitsyn, L. L. Bouilov, and B. V. Deryagin, J. Cryst. Growth **52**, 219 (1981).
[10]X. K. Chen, G. Matera, S. Pramanick, and J. Narayan, in *Proceedings of the Second International Symposium on Diamond Materials,* edited by A. J. Purdes *et al.* (Electrochemical Society, Pennington, NJ, 1991), p. 73.
[11]Y. H. Lee, K. J. Bachmann, J. T. Glass, Y. M. LeGrice, and R. J. Nemanich, Appl. Phys. Lett. **57**, 1916 (1990).
[12]J. E. Field, in *The Properties of Diamond,* edited by J. E. Field (Academic, London, 1979), p. 284.
[13]R. C. Bean, K. R. Zanio, K. A. Hay, J. M. Wright, E. J. Saller, R. Fischer, and H. Morkoc, J. Vac. Sci. Technol. A **4**, 2153 (1986).
[14]R. F. Davis, G. Kelner, M. Shur, J. W. Palmour, and J. A. Edmond, Proc. IEEE **79**, 677 (1991).
[15]H. S. Jin, A. S. Yapsin, T. M. Lu, W. M. Gibson, I. Yamada, and T. Takagi, Appl. Phys. Lett. **50**, 1062 (1987).
[16]K. H. Park, H. S. Jin, L. Luo, W. M. Gibson, G. C. Wang, and T. M. Lu, in *Epitaxy of Semiconductor Layered Structures,* edited by R. T. Tung, L. R. Dawson, and R. L. Gunshor, MRS Symposia Proceedings No. 102 (Materials Research Society, Pittsburgh, 1988), p. 271.
[17]S. Nishino, J. A. Powell, and H. A. Will, Appl. Phys. Lett. **42**, 460 (1983).
[18]S. Nishino, Y. Hazuki, H. Matsunami, and T. Tanaka, J. Electrochem. Soc. **127**, 2674 (1980).
[19]H. S. Kong, Y. C. Wang, J. T. Glass, and R. F. Davis, J. Mater. Res. **3**, 521 (1988).
[20]R. F. Davis and J. T. Glass, in *Advances in Solid-State Chemistry,* edited by C. R. A. Catlow (JAI, London, 1991), Vol. 2, pp. 1–111.
[21]J. T. Glass, P. Richard, Y. H. Lee, H. S. Kong, and K. J. Bachmann (unpublished).
[22]T. Hartnett, R. Miller, D. Montanari, C. Willingham, and R.

Tustison, J. Vac. Sci. Technol. A **8**, 2129 (1990).
[23]B. R. Stoner and J. T. Glass, Appl. Phys. Lett. **60**, 698 (1992).
[24]F. C. Frank and J. H. van der Merwe, Proc. R. Soc. London Ser. A **198**, 205 (1949).
[25]N. H. Fletcher, Philos. Mag. **16**, 159 (1967).
[26]N. H. Fletcher and K. W. Lodge, in *Epitaxial Growth, Part B,* edited by J. W. Matthews (Academic, New York, 1975), p. 529.
[27]H. Reiss, J. Appl. Phys. **39**, 5045 (1968).
[28]J. H. van der Merwe, Philos. Mag. **45**, 127 (1982).
[29]Y. Gotoh and I. Arai, Jpn. J. Appl. Phys. **25**, L583 (1986).
[30]M. W. H. Braun and J. H. van der Merwe, S. African J. Sci. **84**, 670 (1988).
[31]M. W. H. Braun, D. Sc. thesis, University of Pretoria, South Africa, 1987.
[32]B. D. Cullity, *Elements of X-Ray Diffraction* (Addison-Wesley, Reading, MA, 1978), p. 489.
[33]J. H. van der Merwe and M. W. H. Braun, in *Interfaces, Superlattices, and Thin Films,* edited by J. D. Dow and I. K. Schuller, MRS Symposia Proceedings No. 77 (Materials Research Society, Pittsburgh, 1987), p. 133.
[34]J. H. van der Merwe and M. W. H. Braun, Appl. Surf. Sci. **22/23**, 545 (1985).
[35]R. Vanselow, M. W. H. Braun, and J. H. van der Merwe, Surf. Sci. **214**, 197 (1989).
[36]E. Bauer and J. H. van der Merwe, Phys. Rev. B **33**, 3657 (1986).
[37]M. W. Braun, H. S. Kong, J. T. Glass, and R. F. Davis, J. Appl. Phys. **69**, 2679 (1991).
[38]A. R. Badzian, in *Advances in X-Ray Analysis,* edited by C. B. Barrett *et al.* (Plenum, New York, 1988), Vol. 31, p. 113.
[39]B. R. Stoner, B. E. Williams, S. D. Wolter, K. Nishimura, and J. T. Glass, J. Mater. Res. **7**, 257 (1992).
[40]B. R. Stoner, G.-H. M. Ma, S. D. Wolter, and J. T. Glass, Phys. Rev. B **45**, 11 067 (1992).
[41]C. H. Carter, R. F. Davis, and S. R. Nutt, J. Mater. Res. **1**, 811 (1986).
[42]P. M. J. Maree, J. C. Barbour, J. F. van der Veen, K. L. Kavanagh, C. W. T. Bulle-Lieuwma, and M. P. A. Viegers, J. Appl. Phys. **62**, 4413 (1987).
[43]M. Volmer and A. Weber, Z. Phys. Chem. **119**, 277 (1926).
[44]I. N. Stranski and L. Krastanov, Sitzungsber, Akad., Wiss. Wien, Math-Naturewiss. K 1IIb **146**, 797 (1938).
[45]R. F. Davis, J. T. Glass, K. J. Bachmann, and R. J. Trew (unpublished).
[46]W. Zhu, B. R. Stoner, B. E. Williams, and J. T. Glass, Proc. IEEE **79**, 621 (1991).
[47]J. C. Bean, in *Heteroepitaxy on Si II,* edited by J. C. C. Fan, J. M. Phillips, and B. Y. Tsaur, MRS Symposia Proceedings No. 91 (Materials Research Society, Pittsburgh, 1987), p. 269.
[48]J. S. McCalmont, D. Robinson, K. M. Lakin, and H. R. Shanks, in *Heteroepitaxy on Si II* (Ref. 47), p. 323.
[49]J. W. Lee, J. P. Salerno, R. P. Gale, and J. C. C. Fan, in *Heteroepitaxy on Si II* (Ref. 47), p. 33.
[50]N. Otsuka, C. Choi, Y. Nakamura, S. Nagakura, R. Fischer, and H. Morkoc, Appl. Phys. Lett. **49**, 277 (1986).
[51]Z. Liliental-Weber, E. R. Weber, J. Washburn, T. Y. Liu, and H. Kroemer, in *Heteroepitaxy on Si II* (Ref. 47), p. 91.
[52]B. A. Fox and W. A. Jesser, J. Appl. Phys. **68**, 2739 (1990).
[53]J. H. V. d. Merwe, J. Appl. Phys. **34**, 123 (1962).
[54]W. A. Jesser and B. A. Fox, J. Electron. Mater. **19**, 1289 (1990).
[55]W. T. Read, Jr. *Dislocations in Crystals* (McGraw-Hill, New York, 1953), p. 157.
[56]R. J. Matyi, J. W. Lee, and H. F. Schaake, J. Electron. Mater. **17**, 87 (1988).
[57]R. J. Matyi, H. F. Schaake, D. G. Deppe, and J. N. Holonyak, in *Proceedings of the Symposium on Heteroepitaxial Approaches in Semiconductors: Lattice Mismatch and its Consequences,* edited by A. T. Macrander and T. J. Drummond, (Electrochemical Society, Pennington, NJ, 1988), Vol. 89, p. 195.
[58]G. H. Olsen and M. Ettenberg, in *Crystal Growth; Theory and Techniques,* edited by C. H. L. Goodman (Plenum, New York, 1978), Vol. 2.
[59]D. A. Porter and K. E. Easterling, *Phase Transformations in Metals and Alloys* (Van Nostrand Reinhold, New York, 1981), p. 117.
[60]J. P. Hirth and J. Lothe, *Theory of Dislocations* (Wiley, New York, 1982), p. 706.
[61]M. Shigeta, K. Nakanishi, Y. Fujii, K. Furukawa, A. Hatano, A. Uemoto, A. Suzuki, and S. Nakajima, Appl. Phys. Lett. **50**, 1684 (1987).
[62]L. A. Kolodziejski, R. L. Gunshor, N. Otsuka, and C. Choi, J. Vac. Sci. Technol. A **4**, 2150 (1986).
[63]Z. Liliental-Weber, J. Vac. Sci. Technol. B **5**, 1007 (1987).
[64]L. J. Schowalter and R. W. Fathauer, J. Vac. Sci. Technol. A **4**, 1026 (1986).
[65]E. Muller, H. U. Nissen, M. Ospelt, and H. v. Kanel, Phys. Rev. Lett. **63**, 1819 (1989).
[66]J. R. Patel, P. E. Freeland, M. S. Hybertsen, D. C. Jacobson, and J. A. Golvechenko, Phys. Rev. Lett. **59**, 2180 (1987).
[67]H. Zogg and S. Blunier, Appl. Phys. Lett. **49**, 1531 (1986).
[68]R. Hull and J. C. Bean, Semicond. Semimetals **33**, 1 (1991).
[69]M. Copel, M. C. Reuter, E. Kaxiras, and R. M. Tromp, Phys. Rev. Lett. **63**, 632 (1989).

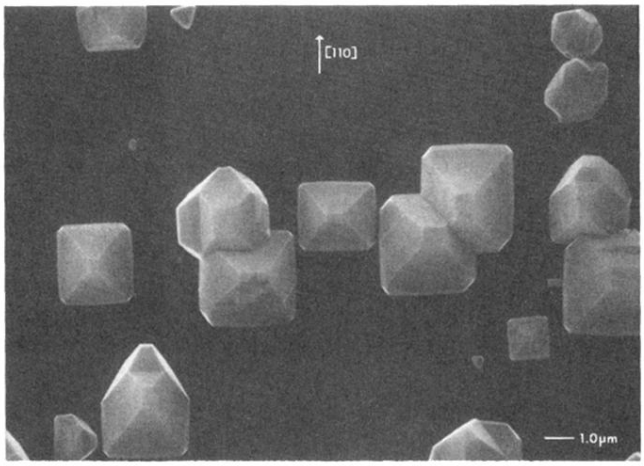

(a)

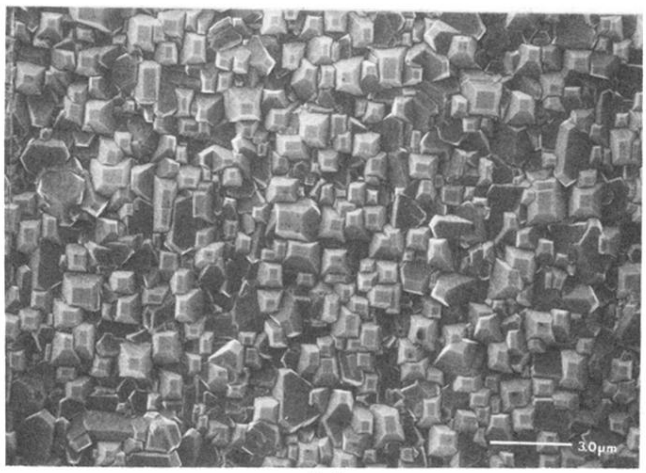

(b)

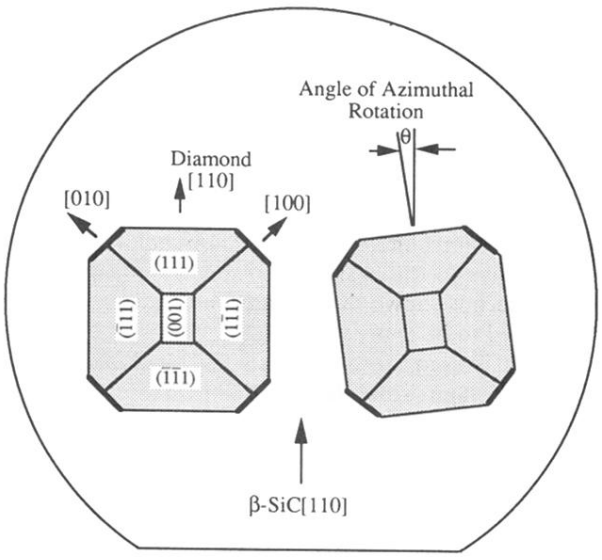

β-SiC (001) Wafer

(c)

FIG. 2. SEM micrographs of textured diamond grains grown on β-SiC substrate taken from (a) the center and (b) the edge of the sample, and (c) is a schematic representation of the orientations of diamond grains with respect to the β-SiC substrate surface.

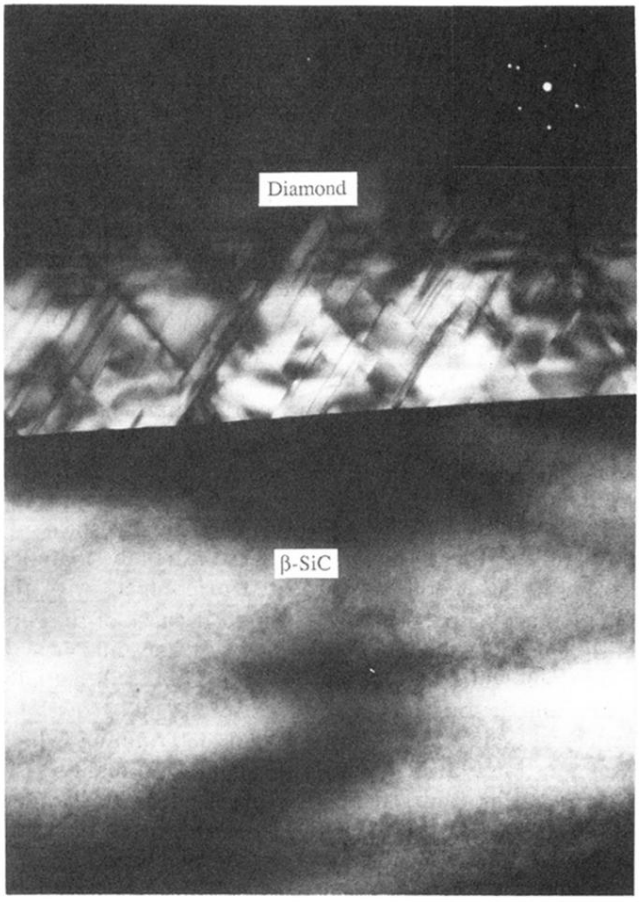

FIG. 3. An XTEM micrograph of the diamond/β-SiC interface and the corresponding TED pattern.

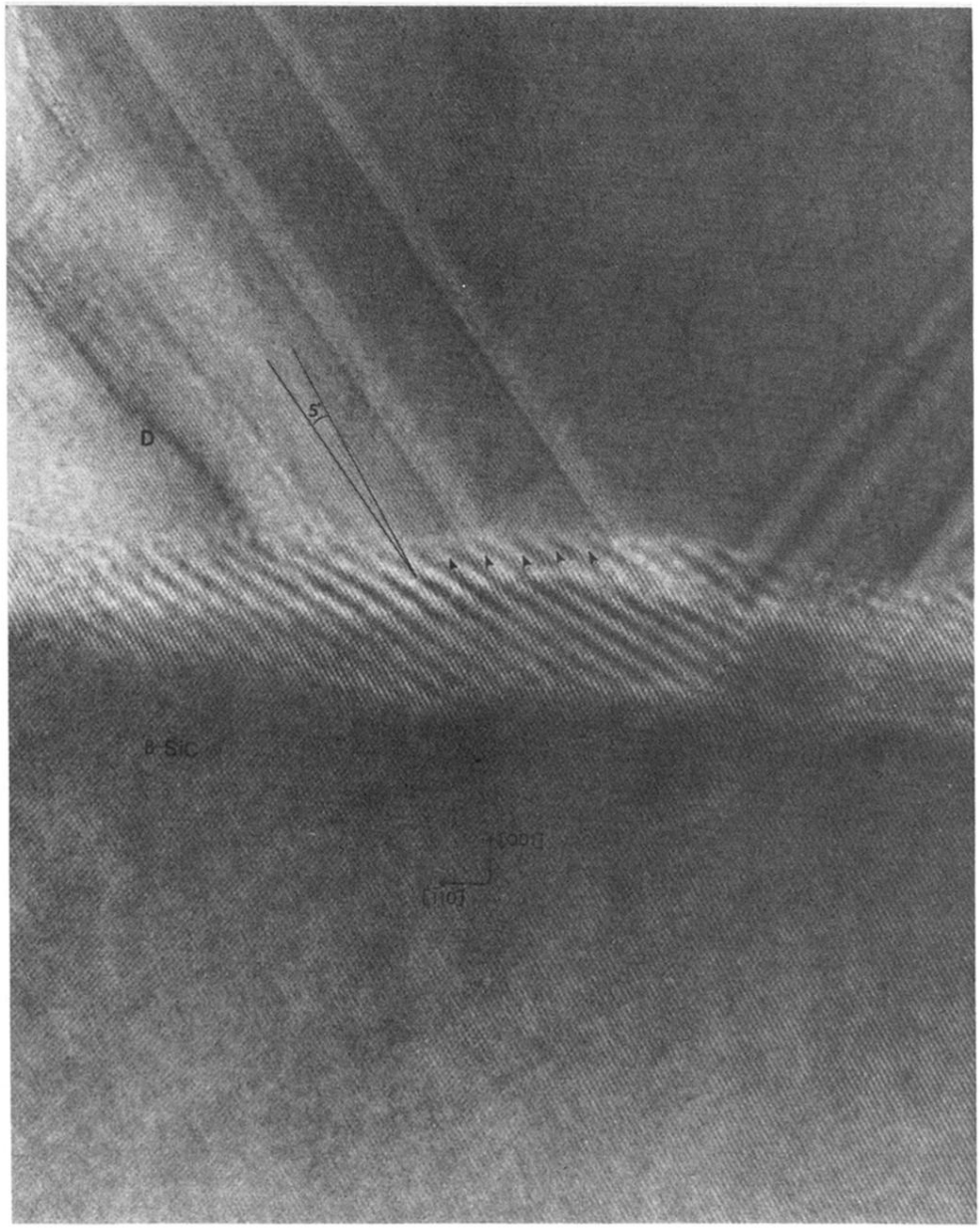

FIG. 5. A HRTEM micrograph of the diamond/β-SiC interface. Arrows indicate the positions of misfit dislocations.